scientific reports

OPEN

A fixed 20:1 combination of cafedrine/theodrenaline increases cytosolic Ca^{2+} concentration in human tracheal epithelial cells via ryanodine receptor-mediated Ca^{2+} release

Götz Schmidt[1✉], Gerrit Rienas[1], Sabrina Müller[1], Katrin Richter[2], Michael Sander[1], Christian Koch[1,4] & Michael Henrich[3,4]

Mucociliary clearance is a pivotal physiological mechanism that protects the lung by cleaning the airways from pollution and colonization, thereby preventing infection. Ciliary function is influenced by various signal transduction cascades, and Ca^{2+} represents a key second messenger. A fixed 20:1 combination of cafedrine and theodrenaline has been widely used to treat perioperative hypotension and emergency hypotensive states since the 1960s; however, its effect on the intracellular Ca^{2+} concentration ($[Ca^{2+}]_i$) of respiratory epithelium remains unknown. Therefore, human tracheal epithelial cells were exposed to the clinically applied 20:1 mixture of cafedrine/theodrenaline and the individual substances separately. $[Ca^{2+}]_i$ was assessed by FURA-2 340/380 fluorescence ratio. Pharmacological inhibitors were applied to elucidate relevant signal transduction cascades, and reverse transcription polymerase chain reaction (RT-PCR) was performed on murine tracheal epithelium to analyze ryanodine receptor (RyR) subtype expression. All three pharmacological preparations instantaneously induced a steep increase in $[Ca^{2+}]_i$ that quickly returned to its baseline value despite the persistence of each substance. Peak $[Ca^{2+}]_i$ following the administration of 20:1 cafedrine/theodrenaline, cafedrine alone, and theodrenaline alone increased in a dose-dependent manner, with median effective concentrations of 0.35 mM (7.32 mM cafedrine and 0.35 mM theodrenaline), 3.14 mM, and 3.45 mM, respectively. When extracellular Ca^{2+} influx was inhibited using a Ca^{2+}-free buffer solution, the peak $[Ca^{2+}]_i$ following the administration of cafedrine alone and theodrenaline alone were reduced but not abolished. No alteration in $[Ca^{2+}]_i$ compared with baseline $[Ca^{2+}]_i$ was observed during β-adrenergic receptor inhibition. Depletion of caffeine-sensitive stores and inhibition of RyR, but not IP$_3$ receptors, completely abolished any increase in $[Ca^{2+}]_i$. However, $[Ca^{2+}]_i$ still increased following the depletion of mitochondrial Ca^{2+} stores using 2,4-dinitrophenol. RT-PCR revealed RyR-2 and RyR-3 expression on murine tracheal epithelium. Although our experiments showed that cafedrine/theodrenaline, cafedrine alone, or theodrenaline alone release Ca^{2+} from intracellular stores through mechanisms that are exclusively triggered by β-adrenergic receptor stimulation, which most probably lead to RyR activation, clinical plasma concentrations are considerably lower than those used in our experiments to elicit an increase in $[Ca^{2+}]_i$; therefore, further studies are needed to evaluate the ability of cafedrine/theodrenaline to alter mucociliary clearance in clinical practice.

[1]Department of Anesthesiology, Operative Intensive Care Medicine and Pain Therapy, Justus Liebig University of Giessen, Rudolf-Buchheim-Strasse 7, 35392 Giessen, Germany. [2]Department of General and Thoracic Surgery, Justus Liebig University of Giessen, Rudolf-Buchheim-Strasse 7, 35392 Giessen, Germany. [3]Department of Anesthesiology, Intensive Care Medicine, Emergency Medicine, Vidia St. Vincentius-Clinic Karlsruhe gAG, Karlsruhe, Germany. [4]These authors jointly supervised this work: Christian Koch and Michael Henrich. ✉email: Goetz.F.Schmidt@chiru.med.uni-giessen.de

Abbreviations

2-APB	2-Aminoethoxydiphenylborane
$[Ca^{2+}]_i$	Intracellular Ca^{2+} concentration
cAMP	Cyclic adenosine monophosphate
cGMP	Cyclic guanosine monophosphate
DMSO	Dimethyl sulfoxide
DNP	2,4-Dinitrophenol
EC_{50}	Median effective concentration
ER	Endoplasmic reticulum
HEPES	4-(2-Hydroxyethyl)-1-piperazineethanesulfonic acid
IP_3	Inositol trisphosphate
KCl	Potassium chloride
mRNA	Messenger ribonucleic acid
PDE	Phosphodiesterases
RT-PCR	Reverse transcription polymerase chain reaction
RyR	Ryanodine receptor
SERCA	Sarcoplasmic/endoplasmic reticulum calcium ATPase
SOCE	Store-operated Ca^{2+} entry

Mucociliary clearance of the lower airways is a pivotal physiological mechanism that protects the lung by clearing the airways of pollution and colonization by pathogens, thereby preventing infection. Together with basal, suprabasal, and goblet cells, multiciliated epithelial cells constitute the complex mucociliary clearance function of the respiratory tract[1]. Ciliary cells prevent the accumulation of debris and colonization by microbial pathogens via an outward-directed transportation processes[1,2]. Cilia are hair-like protrusions located on the apical side of the respiratory epithelium along the airways; they are composed of unique structural proteins, including motor proteins, like the ATP-dependent dynein[2,3]. Due to their continuous synchronized and orally directed motion, inhaled particles and complex compositions of mucus, electrolytes, and endogenous defensive substances are removed from the lower airways and are subsequently coughed up under normal physiological conditions[1,4]. While the ciliary apparatus continuously beats without external stimulation, various events can provoke an increase in ciliary beating frequency, when necessary[1,4]. Exogenous, endogenous, and paracrine effects moderate ciliary activity, and Ca^{2+} functions as a central second messenger. Therefore, intracellular Ca^{2+} concentration ($[Ca^{2+}]_i$) represents a keystone regulating ciliary activity because most signal transduction cascades, which contribute to the ciliary beating frequency, induce at least a temporary increase in $[Ca^{2+}]_i$[1,4,5]. Intracellular Ca^{2+} is foremost stored in the endoplasmic reticulum (ER) and is released following inositol trisphosphate (IP_3) or ryanodine receptor (RyR) activation[3]. Furthermore, the ER regulates $[Ca^{2+}]_i$ via the sarcoplasmic/endoplasmic reticulum calcium ATPase (SERCA), which pumps cytosolic Ca^{2+} ions to its internal stores, maintaining the balance of $[Ca^{2+}]_i$[6,7]. Mitochondria also contribute to intracellular Ca^{2+} homeostasis by buffering Ca^{2+} ions when $[Ca^{2+}]_i$ exceeds a threshold of 500 nM[8,9]. In addition, other cell organelles contribute to intracellular Ca^{2+} homeostasis, such as lysosomes, which contain Ca^{2+} but can also regulate mitochondrial Ca^{2+} dynamics, and peroxisomes; however, their individual influence on $[Ca^{2+}]_i$ in ciliary cells and mucociliary clearance remains unknown[6,10,11]. $[Ca^{2+}]_i$ is not only increased by Ca^{2+} release from intracellular stores; extracellular Ca^{2+} can enter the cell via plasma membrane-bound Ca^{2+} channels. Although voltage-gated calcium channels and transient receptor potential channels are located at the plasma membrane together, the predominant method of extracellular Ca^{2+} entry into non-excitable cells occurs via store-operated Ca^{2+} entry (SOCE)[12,13]. SOCE is triggered by an increase in $[Ca^{2+}]_i$ that is predominantly caused by the liberation of Ca^{2+} from internal stores[12]. Stromal interaction molecule proteins are located at the ER membrane, and they activate SOCE when Ca^{2+} is released[12,13]. Therefore, changes in $[Ca^{2+}]_i$ produce fundamental metabolic and functional alterations in ciliary cells and can be influenced by different drugs administered in various settings.

In Germany, intraoperative hypotension and emergency hypotensive states have been treated with a combination of cafedrine and theodrenaline (Akrinor®, Ratiopharm GmbH, Ulm, Germany) since the 1960s[14–16]. Covalently linked theophylline and norephedrine compose cafedrine, and theodrenaline is formed from theophylline and noradrenaline in the same manner[14,17]. Both compounds are administered in a fixed 20:1 combination of cafedrine and theodrenaline as an intravenous bolus in adults, and they restore mean arterial blood pressure by increasing preload, cardiac stroke volume, and cardiac output[14,15,18]. The clinical effects of cafedrine/theodrenaline are mediated through β_1-adrenoreceptor and α-adrenoreceptor stimulation, and nonspecific inhibition of phosphodiesterases (PDEs) is believed to enhance their response[14,17]. In contrast with synthetic vasopressors (e.g., ephedrine, phenylephrine), systemic vascular resistance and heart rate remain mostly unaffected, which makes cafedrine/theodrenaline especially appealing in obstetric surgery[14,16,19]. Although cafedrine/theodrenaline has been widely used for decades, little is known about its pharmacodynamics or pharmacokinetics in specific end organs[14,16]. This is surprising as the unique combination of three single drugs (theophylline, norephedrine, noradrenaline) in a 20:1 mixture might produce different effects in vivo as recently shown in human atrial myocardium and internal mammary arteries[17]. However, the influence of cafedrine/theodrenaline on the $[Ca^{2+}]_i$ of human respiratory cilia cells has not yet been investigated. The aim of this study was to evaluate the influence of cafedrine/theodrenaline on the $[Ca^{2+}]_i$ of human tracheal epithelial cells. Cells were exposed to the clinically used 20:1 mixture of cafedrine/theodrenaline and the individual substances alone. Our experiments elucidated the effects of the individual components and identified the relevant pharmacological signaling cascades leading to alterations in $[Ca^{2+}]_i$. Therefore, we applied specific inhibitory substances inhibiting distinct signal transduction cascades, and we evaluated the origin of the released Ca^{2+}. Furthermore, we used reverse transcription

polymerase chain reaction (RT-PCR) to detect the messenger ribonucleic acid (mRNA) expression of key receptor subtypes influencing $[Ca^{2+}]_i$ following the administration of cafedrine/theodrenaline, cafedrine alone, and theodrenaline alone.

Methods

Drugs and buffer solutions

The historically established 20:1 ratio of cafedrine/theodrenaline refers to mass, not molarity. Therefore, due to the different molar masses of cafedrine (357.41 g/mol) and theodrenaline (375.38 g/mol), a 1 M solution of cafedrine/theodrenaline 20:1 with a molar mass of 7,882.98 g/mol consists of 1 M theodrenaline and approximately 21 M of cafedrine. Experiments were performed in HEPES solution consisting of 10 mM HEPES, 2.6 mM KCl, 2.5 mM $CaCl_2$, 10 mM glucose, 125 mM NaCl, 1.2 mM KH_2PO_4, and 1.2 mM $MgSO_4$. NaOH was used to adjust the pH to 7.4 at 30 °C. To realize experiments in Ca^{2+}-free solutions, $CaCl_2$ was substituted with 1 mM ethylene glycol tetraacetic acid. The following drugs were applied during the experiments: 2-aminoethoxydiphenylborane (2-APB, 40 µM diluted in 4 µl dimethyl sulfoxide [DMSO], TOCRIS Bioscience, Bristol, UK), 2,4-dinitrophenol (DNP, 25 µM diluted in 10 µl DMSO, Sigma-Aldrich, St. Louis, USA), cafedrine (3.14 mM diluted in 50 µl H_2O, Arevipharma, Radebeul, Germany), cafedrine/theodrenaline 20:1 (0.38 mM diluted in 50 µl H_2O, Akrinor®, Ratiopharm, Ulm, Germany), caffeine (30 mM, Roth, Karlsruhe, Germany), FURA-2 AM (2.5 µM diluted in 5 µl H_2O, Biotium, Fremont, USA), ICI-118,551 (100 µM diluted in 10 µl H_2O, TOCRIS Bioscience, Bristol, UK), KCl (200 mM diluted in 66.6 µl H_2O), ryanodine (40 µM diluted in 16 µl DMSO, TOCRIS Bioscience, Bristol, UK), and theodrenaline (3.45 mM diluted in 50 µl H_2O, Arevipharma, Radebeul, Germany). The stated drug concentrations were achieved during the experiments after applying the stock solution to the buffer solution in the recording chamber. In control experiments, the buffer solution or the solvent alone was applied to rule out any contribution of the buffer, the solvent, or the mechanical application process to the Ca^{2+} signals.

Calcium imaging in isolated human tracheal epithelial cells

Human tracheal epithelial cells (HTEpC, C12644, PromoCell, Heidelberg, Germany) were cultured with the Airway Epithelial Growth Medium Kit (C-21160) containing the Airway Epithelial Growth Medium Supplement Pack (C-39160, both PromoCell, Heidelberg, Germany) in a humidified chamber at 37 °C with air containing 5% CO_2. Cells from passage one to three were seeded onto laminin-coated coverslips for $[Ca^{2+}]_i$ measurements in 4-(2-hydroxyethyl)-1-piperazineethanesulfonic acid (HEPES) buffer. Dye loading was performed in the dark with 2.5 µM FURA-2 AM for 45 min at 37 °C. The cell-containing coverslip was then rinsed in fresh HEPES buffer and subsequently transferred to the recording chamber of an upright fluorescence microscope equipped with a 20 × immersion lens (BX50 WI, Olympus, Hamburg, Germany), where the coverslip was placed into a Delta T culture dish (Bioptechs, Butler, USA) containing 2 ml of fresh HEPES buffer. Excitation light was provided by a 50 W xenon lamp, and the microscope was equipped with a dichroic excitation longpass mirror at 400 nm. FURA-2 AM was excited at 340 nm and 380 nm while equipped with bandpass excitation filters. The emitted fluorescence was directed through a dichroic shortpass filter of 560 nm to a bandpass filter of 510 nm and was recorded with a scientific camera (SMX-150, Sumix, Oceanside, USA). Measurements of the FURA-2 AM 340/380 ratio were performed every second for 1,000 s using an automated protocol of the TiLLvisION Imaging software program (Till Photonics, Gräfeling, Germany). Cafedrine, theodrenaline, or 20:1 cafedrine/theodrenaline were added following a 100-s resting period to ensure adequate baseline calibration. After 800 s, 200 mM potassium chloride (KCl) was added to the buffer solution to completely invert the membrane potential, leading to massive influx of Ca^{2+} indicating the integrity of the analyzed cells up to the end of the respective experiment.

RNA extraction from murine tissues

Male C57BL6J mice (n = 5) weighing 25–35 g (aged 12–15 weeks) were purchased from Charles River (Sulzfeld, Germany) to characterize the expression of RyR in the respiratory epithelium. All procedures involving animals were conducted in compliance with the European legislation for the protection of animals used for scientific purposes, the ARRIVE guidelines and the standards for animal experiments according to the German animal welfare law and were approved by the local committee for animal care of the regional council of Giessen, Germany (Permit number 813_M, Regional Council of Giessen, Germany). After deep narcosis using 5% isoflurane (Baxter, Unterschleissheim, Germany), animals were sacrificed by cervical dislocation. Tracheae, tracheal epithelium, diaphragm, cardiac muscle, and skeletal muscle were subsequently collected. To obtain isolated tracheal epithelium, the epithelial layer was gently scrubbed from the opened trachea using a hygienic swab. All tissues were stored in RNA stabilization lotion (Invitrogen™ RNAlater™, Thermo Fisher Scientific, Waltham, USA) at − 20 °C until further processing. Tissue probes were then lysed in 350 µl RNeasy Lysis Buffer (Qiagen, Hilden, Germany) containing 3.5 µl ß-mercaptoethanol and they were subsequently homogenized in a tissue homogenizer (Precellys Evolution homogenizer, Bertin Technologies, Montigny-le-Bretonneux, France). RNA was extracted using the RNeasy Micro Kit, and DNA removal was performed using the RNase-Free DNase set (both Qiagen, Hilden, Germany).

RT-PCR

cDNA synthesis was performed using the QuantiTect Reverse Transcription Kit (Qiagen, Hilden, Germany) according to the manufacturer's protocol and stored at − 20 °C until further use. RyR-1, RyR-2, and RyR-3 expression in whole trachea and in the respiratory epithelium alone (each n = 5) was analyzed using specific primers at temperatures shown in Table 1. Primers were selected using the NCBI Primer designing tool (https://www.ncbi.nlm.nih.gov/tools/primer-blast, National Institutes of Health, Bethesda, MD, USA). Skeletal muscle (RyR-1), cardiac muscle (RyR-2), and diaphragm (RyR-3) served as positive controls, and H_2O was used as negative control.

Target	Gene	Sequence	Product length (bp)	Annealing temperature (°C)
RyR 1	*Ryr1*	Forward: 5'-CGCTCCCACTTCATCCCTAC-3'	385	55
		Reverse: 5'-CTCCTGCCTTGGCCATTTTG-3'		
RyR 2	*Ryr2*	Forward: 5'-ACCTACTCCGAAGGCTGGTGTT-3'	148	55
		Reverse: 5'-TTCTTCCGAGGCAGCACCAAAG-3'		
RyR 3	*Ryr3*	Forward: 5'-GACAGGACCAGGAACGGAAG-3'	315	58
		Reverse: 5'-GCTCCACCGTCTTTTCTGGA-3'		

Table 1. List of murine ryanodine receptor (RyR) primers used for RT-PCR and their specific annealing temperatures.

Primer concentration was set at 0.2 μM and reactions were performed in a Mastercycler gradient (Eppendorf, Hamburg, Germany). TAQ polymerase (Qiagen, Hilden, Germany) was activated at 95° for 3 min, followed by 40 cycles consisting of a 1-min denaturation step at 95 °C, a 45-s annealing step at a primer-specific temperature (Table 1), and a 3-min extension step at 72 °C. PCR products were visualized using GelRed (Biotium, Fremont, CA, USA) with a digital imaging system (Vilber Lourmat, Eberhardzell, Germany) in agarose gel (1% TAE buffer) after electrophoresis at 100 V for 80 min. GeneRuler 100 bp (Thermo Fisher Scientific, Waltham, USA) was used to verify the proper size of the PCR products.

Statistical analysis
FURA-2 340/380 ratio was recorded from at least 30 cells per experimental setup. These 30 cells were collected from at least three different coverslips each evaluating 10 cells taken from cell passages one to three. Measurements were only included in the statistical analyses when clear response of the FURA-2-fluorescence ratio (doubling of the ratio) was detected after the application of KCl at the end of the experiments. Median effective concentrations (EC_{50}) were calculated using the Hill equation. The Mann–Whitney U test was used to compare the peak measurement points from different experiments, while the Wilcoxon rank sum test was used to compare paired variables. In general, two-tailed values of $p < 0.05$ were considered statistically significant, while multiple comparison problems were counteracted by adjusting the α-level according to the Bonferroni correction. GraphPad PRISM (Version 9.5.0, GraphPad Software, La Jolla, CA, USA) was used for statistical analysis and figure creation.

Ethical approval
Permit number 813_M, Regional Council of Giessen, Germany.

Results
20:1 cafedrine/theodrenaline, cafedrine, and theodrenaline induce a transient rise in $[Ca^{2+}]_i$
Under resting conditions, FURA-2 340/380 ratio remained constant during the whole observation period (FURA-2 340/380 ratio: 0.98 ± 0.02, Fig. 1). $[Ca^{2+}]_i$, indicated by FURA-2 340/380 ratio, sharply increased when KCl was applied at the end of the experiments, indicating the vitality of the human tracheal epithelial cells. This is demonstrated for all the experiments by an example in Fig. 1. Application of 20:1 cafedrine/theodrenaline, cafedrine alone, and theodrenaline increased $[Ca^{2+}]_i$ in a dose-dependent manner following the Hill equation (Fig. 2A,C,E). EC_{50} calculated for 20:1 cafedrine/theodrenaline, cafedrine, and theodrenaline were 0.35 mM (2.75 mg/ml consisting of 2.62 mg/ml [7.32 mM] cafedrine and 0.13 mg/ml [0.35 mM] theodrenaline), 3.14 mM (1.12 mg/ml), and 3.45 mM (1.30 mg/ml), respectively. All three substances provoked a sharp increase in $[Ca^{2+}]_i$ that was observed immediately, within 5 s after application (FURA-2 340/380 ratios of cafedrine/theodrenaline: 1.76 ± 0.06, cafedrine: 4.06 ± 0.24, theodrenaline: 4.38 ± 0.31; each $p < 0.001$; Fig. 2B,D,F). $[Ca^{2+}]_i$ subsequently returned to its baseline value despite the ongoing presence of the applied substances, and the steepest decrease was observed after the administration of cafedrine (Fig. 2D). The following experiments aimed to evaluate the proportion of extracellular Ca^{2+} entry contributing to the transient rise in $[Ca^{2+}]_i$.

The increase in $[Ca^{2+}]_i$ depends on extracellular Ca^{2+} entry
$[Ca^{2+}]_i$ of HTEpC assessed in Ca^{2+}-free buffer solution remained constant under resting conditions (FURA-2 340/380 ratio: 1.00 ± 0.01). Application of 20:1 cafedrine/theodrenaline, cafedrine alone, and theodrenaline alone provoked a significant increase in $[Ca^{2+}]_i$ (FURA-2 340/380 ratio cafedrine/theodrenaline: 1.76 ± 0.06, cafedrine: 1.78 ± 0.24, theodrenaline: 2.68 ± 0.22; each $p < 0.001$; Fig. 3A,C,E). However, compared with Ca^{2+}-containing buffer, peak $[Ca^{2+}]_i$ was significantly lower following the administration of cafedrine and theodrenaline alone (each $p < 0.001$, Fig. 3D,F), while peak $[Ca^{2+}]_i$ of 20:1 cafedrine/theodrenaline was comparable ($p = 0.350$, Fig. 3B). Interestingly, the theodrenaline-induced transient increase in $[Ca^{2+}]_i$ remained elevated and did not reach baseline during the rest of the observation period (Fig. 3E). β-adrenergic receptor stimulation leading to the transient increase in $[Ca^{2+}]_i$ was evaluated in subsequent experiments. Because the relevant influence of extracellular Ca^{2+} entry could not be ruled out following these experiments, all the subsequent experiments were performed in a Ca^{2+}-free buffer solution.
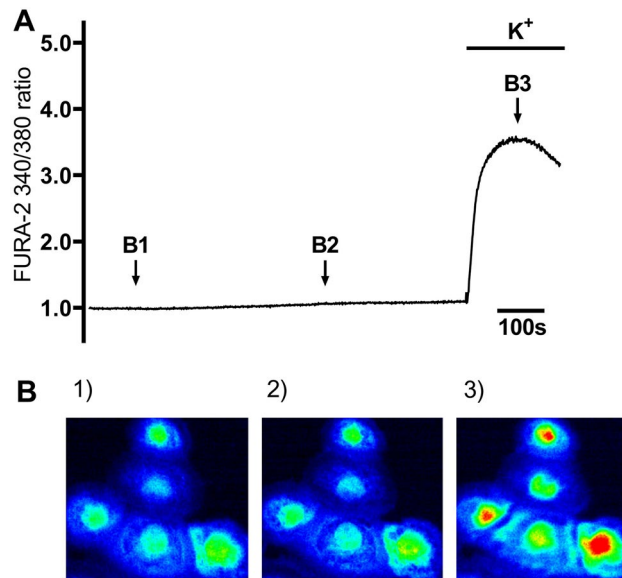
Figure 1. Intracellular Ca^{2+} measurements were performed on Human tracheal epithelial cells (HTEpC). Intracellular Ca^{2+} concentrations ($[Ca^{2+}]_i$) were recorded as Fura-2/AM (Fura-2) fluorescence intensity ratio of 340:380 nm excitation. (**A**) When FURA-2 340/380 ratio was normalized after a 100-s resting period, fluorescence ratio remained constant under resting conditions during the 800-s observation period, demonstrating no changes in $[Ca^2]_i$. Arrows indicate different timepoints of the FURA-2 340/380 ratio, which are illustrated in (**B1–B3**) after conversion into false colors. Potassium chloride (K^+, 200 mM) completely inverted the membrane potential, leading to a strong increase in FURA-2 340/380 fluorescence of human tracheal epithelial cells.

Adrenergic receptor stimulation is responsible for the rise in $[Ca^{2+}]_i$

When the non-selective blocker of β-adrenergic receptors, ICI-118,551 (100 µM), was applied, baseline $[Ca^{2+}]_i$ remained unaltered compared to the Ca^{2+}-free controls (Fig. 4). However, 20:1 cafedrine/theodrenaline, cafedrine alone, and theodrenaline did not provoke any significant alteration in $[Ca^{2+}]_i$ in the presence of ICI-118,551 (cafedrine/theodrenaline: 1.05 ± 0.04, $p = 0.416$, Fig. 4A,B; cafedrine: 0.99 ± 0.01, $p = 0.043$ did not reach the adjusted α-level of 0.013, Fig. 4C,D; theodrenaline: 1.07 ± 0.10, $p = 0.919$, Fig. 4E,F). Because clinically relevant effects of other receptors or PDE could not be assumed from these data, further experiments elucidating these mechanisms were waived.

Ca^{2+} is liberated from ER but not the mitochondria

Because our experiments indicated intracellular Ca^{2+} release, further experiments were conducted to evaluate the origin of the intracellular Ca^{2+}. First, mitochondrial Ca^{2+} stores were depleted using DNP (25 µM, Fig. 5). A small increase in $[Ca^{2+}]_i$ was observed following the administration of DNP, which quickly returned to its baseline; however, 20:1 cafedrine/theodrenaline, cafedrine alone, and theodrenaline alone still provoked a significant increase in $[Ca^{2+}]_i$ (cafedrine/theodrenaline: 1.17 ± 0.05, $p < 0.001$, Fig. 5A,B; cafedrine: 1.24 ± 0.16, $p < 0.001$, Fig. 5C,D; theodrenaline: 2.71 ± 0.27, $p < 0.001$, Fig. 5E,F). While peak values of $[Ca^{2+}]_i$ were comparable after the administration of theodrenaline ($p = 0.994$), 20:1 cafedrine/theodrenaline, and cafedrine alone, $[Ca^{2+}]_i$ peaks were significantly higher in the presence of DNP compared with the $[Ca^{2+}]_i$ peaks without depletion of mitochondrial Ca^{2+} stores (both $p < 0.001$). $[Ca^{2+}]_i$ did not reach baseline following the administration of cafedrine alone or theodrenaline alone. Furthermore, caffeine-sensitive Ca^{2+} stores, which are mainly represented by the ER, were depleted using caffeine (30 mM, Fig. 6). After caffeine was applied, a significant reduction in baseline $[Ca^{2+}]_i$ was observed, indicating Ca^{2+} store depletion (cafedrine/theodrenaline: 0.88 ± 0.01; cafedrine: 0.91 ± 0.01; theodrenaline: 0.90 ± 0.01; each $p < 0.001$). Subsequent application of 20:1 cafedrine/theodrenaline, cafedrine alone, or theodrenaline alone did not increase $[Ca^{2+}]_i$ (cafedrine/theodrenaline: 0.88 ± 0.01, $p = 0.034$ did not reach the adjusted α-level of 0.013, Fig. 6A,B; cafedrine: 0.91 ± 0.01, $p = 0.114$, Fig. 6C,D; theodrenaline: 0.93 ± 0.02; $p = 0.299$, Fig. 6E,F). Because the ER is a crucial caffeine-sensitive Ca^{2+} store, further experiments were conducted to evaluate the signal cascades triggering Ca^{2+} release from these stores.

Increase in $[Ca^{2+}]_i$ is induced by RyR but not IP$_3$ receptor activation

IP$_3$ receptors were inhibited using 2-APB (40 µM, Fig. 7). While 2-APB did not alter baseline $[Ca^{2+}]_i$, application of 20:1 cafedrine/theodrenaline, cafedrine alone, or theodrenaline alone increased $[Ca^{2+}]_i$ to values at least equivalent to $[Ca^{2+}]_i$ without IP$_3$ receptor inhibition (cafedrine/theodrenaline: 1.75 ± 0.08, $p = 0.042$ did not reach the adjusted α-level of 0.013, Fig. 7A,B; cafedrine: 2.58 ± 0.29, $p < 0.001$, Fig. 7C,D; theodrenaline: 2.39 ± 0.29, $p = 0.173$, Fig. 7E,F). In contrast, when RyR were inhibited using ryanodine (40 µM, Fig. 8), the increase in $[Ca^{2+}]_i$
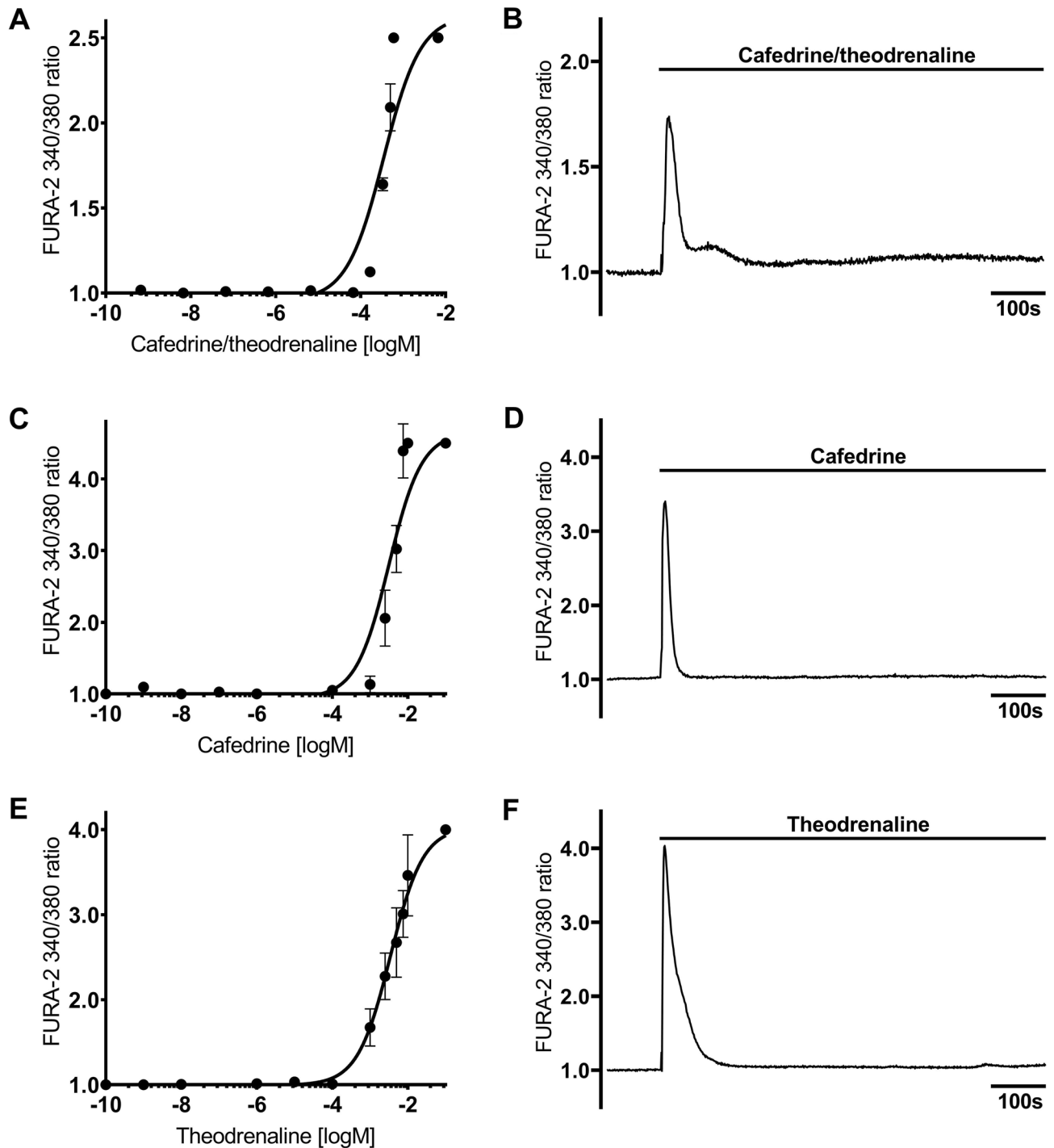
Figure 2. $[Ca^2]_i$ is increased by cafedrine/theodrenaline, cafedrine alone, and theodrenaline alone. Dose–response relationships of (**A**) 20:1 cafedrine/theodrenaline, (**C**) cafedrine alone, and (€) theodrenaline are described by the Hill equation. (**B**) Cafedrine/theodrenaline (0.38 mM), (**D**) cafedrine alone (3.14 mM), and (**F**) theodrenaline alone (3.45 mM) induced a steep increase in $[Ca^2]_i$; however, $[Ca^2]_i$ rapidly returned to its baseline value despite the continued presence of the applied substances. Application of potassium chloride (200 mM) confirmed the vitality of the included cells (not shown). FURA-2 340/380 ratio was normalized after a 100-s resting period, and each group consists of 30 cells from at least three different coverslips, ensuring independent measurements. Scale bar width represents 100 s. ⊥ SEM.

following the application of cafedrine/theodrenaline, cafedrine alone, or theodrenaline alone vanished (cafedrine/theodrenaline: 1.02 ± 0.03, $p = 0.416$, Fig. 8A,B; cafedrine: 1.00 ± 0.01, $p = 0.516$, Fig. 8C,D; theodrenaline: 1.02 ± 0.01, $p = 0.349$, Fig. 8E,F). Because RyR activation was shown to be the crucial mechanism leading to Ca^{2+}
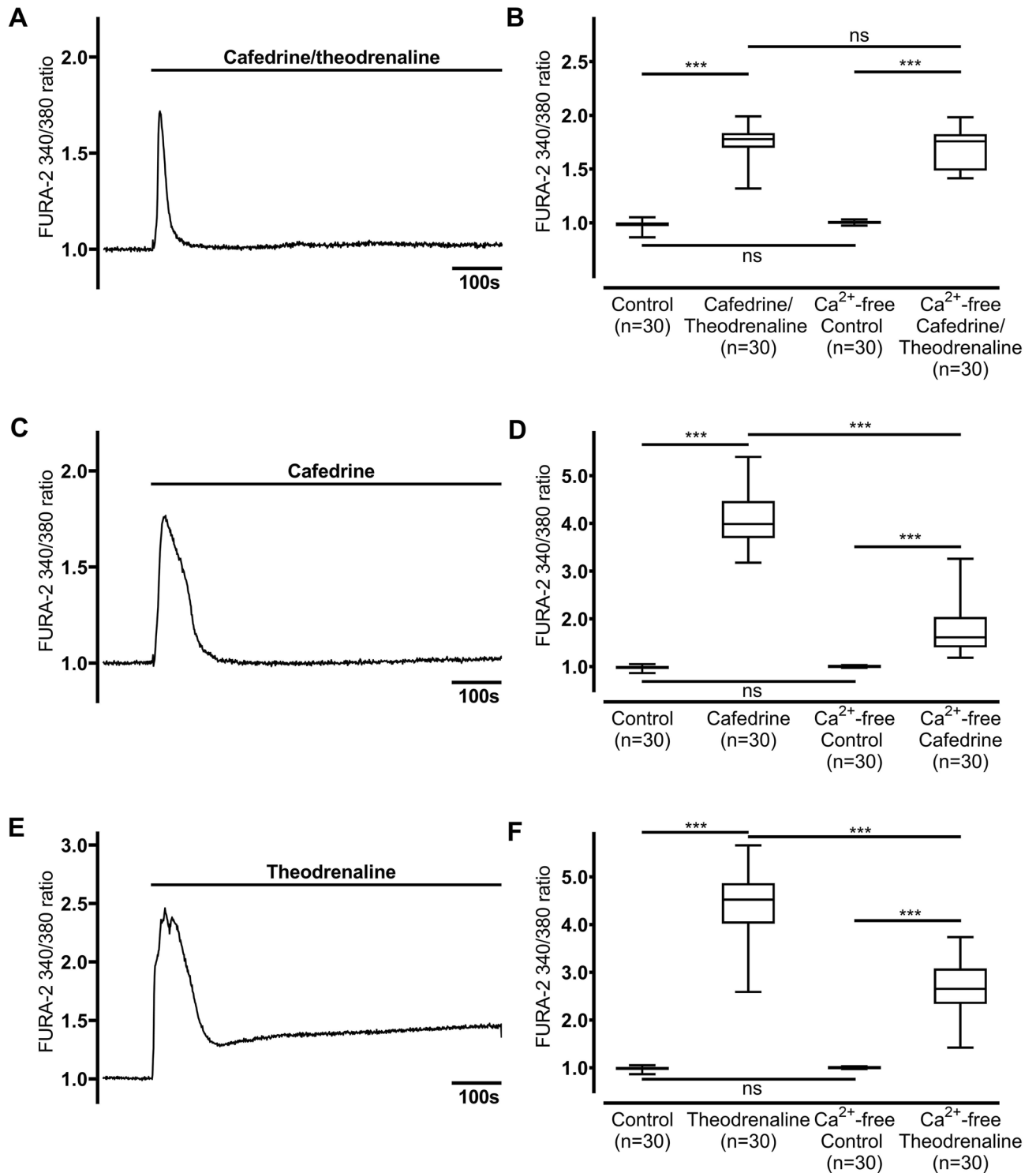
Figure 3. Increase in $[Ca^2]_i$ depends on extracellular Ca^{2+} influx following the application of cafedrine alone or theodrenaline alone. When experiments were performed in Ca^2-free buffer, the maximum $[Ca^2]_i$ provoked by (**A, B**) 20:1 cafedrine/theodrenaline was comparable to the peak $[Ca^2]_i$ seen in Ca^{2+}-containing buffer; however, peak $[Ca^2]_i$ observed after the application of (**C, D**) cafedrine alone and (**E, F**) theodrenaline alone was significantly reduced. When theodrenaline was applied, $[Ca^2]_i$ did not return to its baseline value during the whole observation period. Subsequent application of potassium chloride (200 mM) confirmed the vitality of the included cells (not shown). The control group is represented by the same 30 cells in each chart. FURA-2 340/380 ratio was normalized after a 100-s resting period, and each group consists of 30 cells from at least three different coverslips, ensuring independent measurements. Scale bar width represents 100 s. n = number of individual cells, ***$p < 0.001$, ns: not significant, Mann–Whitney U test, adjusted α-level = 0.013. ⊥ SEM, box and whisker plots indicate median, interquartile range (box), minimum and maximum (whiskers).
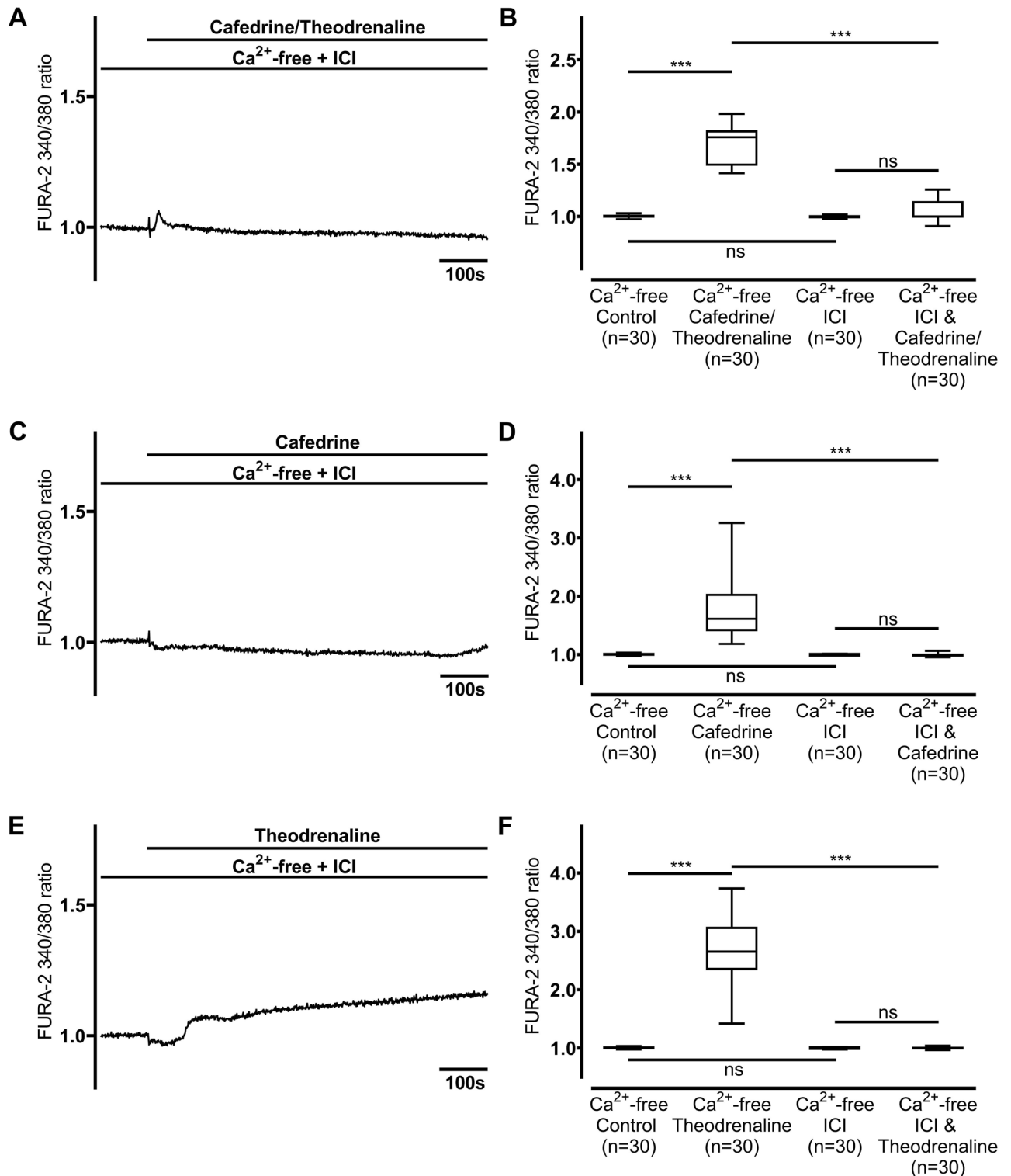
Figure 4. Ca^{2+} release is completely dependent on adrenergic receptor activation. When β-adrenergic receptors were blocked by high concentrations of the non-selective inhibitor ICI-118,551 (100 µM), no relevant peak $[Ca^2]_i$ was observed after the application of (**A, B**) 20:1 cafedrine/theodrenaline, (**C, D**) cafedrine alone, or (**E, F**) theodrenaline alone. The Ca^{2+}-free control group is represented by the same 30 cells in each chart. FURA-2 340/380 ratio was normalized after a 100-s resting period, and each group consists of 30 cells from at least three different coverslips, ensuring independent measurements. Scale bar width represents 100 s. n = number of individual cells, ***$p < 0.001$, ns: not significant, Wilcoxon rank sum test was used to assess ICI-118,551 alone vs. drug preparation during inhibition, otherwise Mann–Whitney U test, adjusted α-level = 0.013. ⊥ SEM, box and whisker plots indicate median, interquartile range (box), minimum and maximum (whiskers).
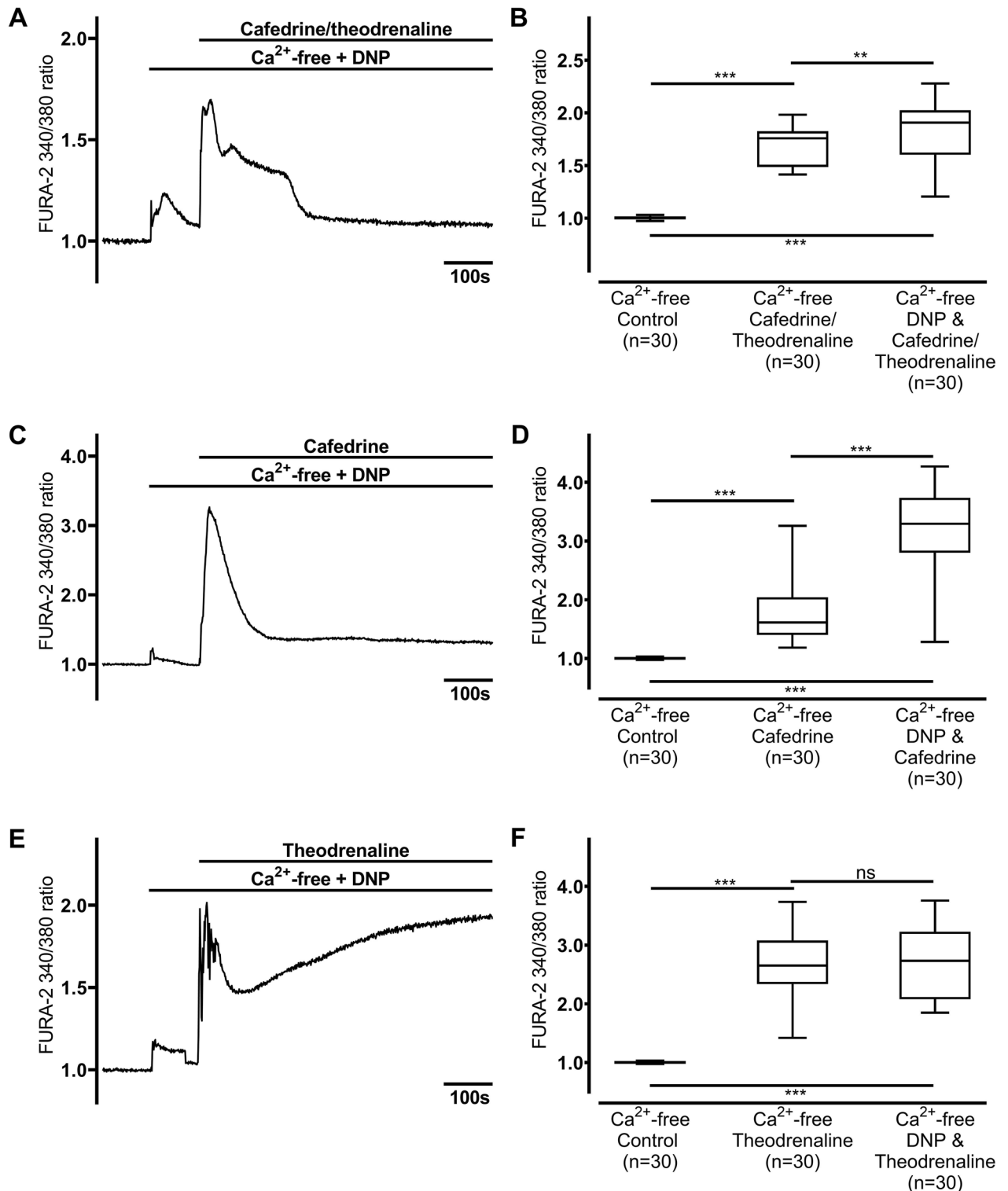
Figure 5. Ca^{2+} release occurs independently from mitochondrial Ca^{2+} stores. When mitochondrial stores were depleted by 2,4-dinitrophenol (DNP, 25 μM), $[Ca^{2+}]_i$ sharply increased following the application of (**A, B**) 20:1 cafedrine/theodrenaline, (**C, D**) cafedrine alone, and (**E, F**) theodrenaline alone. $[Ca^{2+}]_i$ did not return to its baseline value within the observation period. The Ca^{2+}-free control group was represented by the same 30 cells in each chart. FURA-2 340/380 ratio was normalized after a 100-s resting period, and each group consists of 30 cells from at least three different coverslips, ensuring independent measurements. Scale bar width represents 100 s. n = number of individual cells, ***$p < 0.001$, ns: not significant, Mann–Whitney U test, adjusted α-level = 0.017. ⊥ SEM, box and whisker plots indicate median, interquartile range (box), minimum and maximum (whiskers).
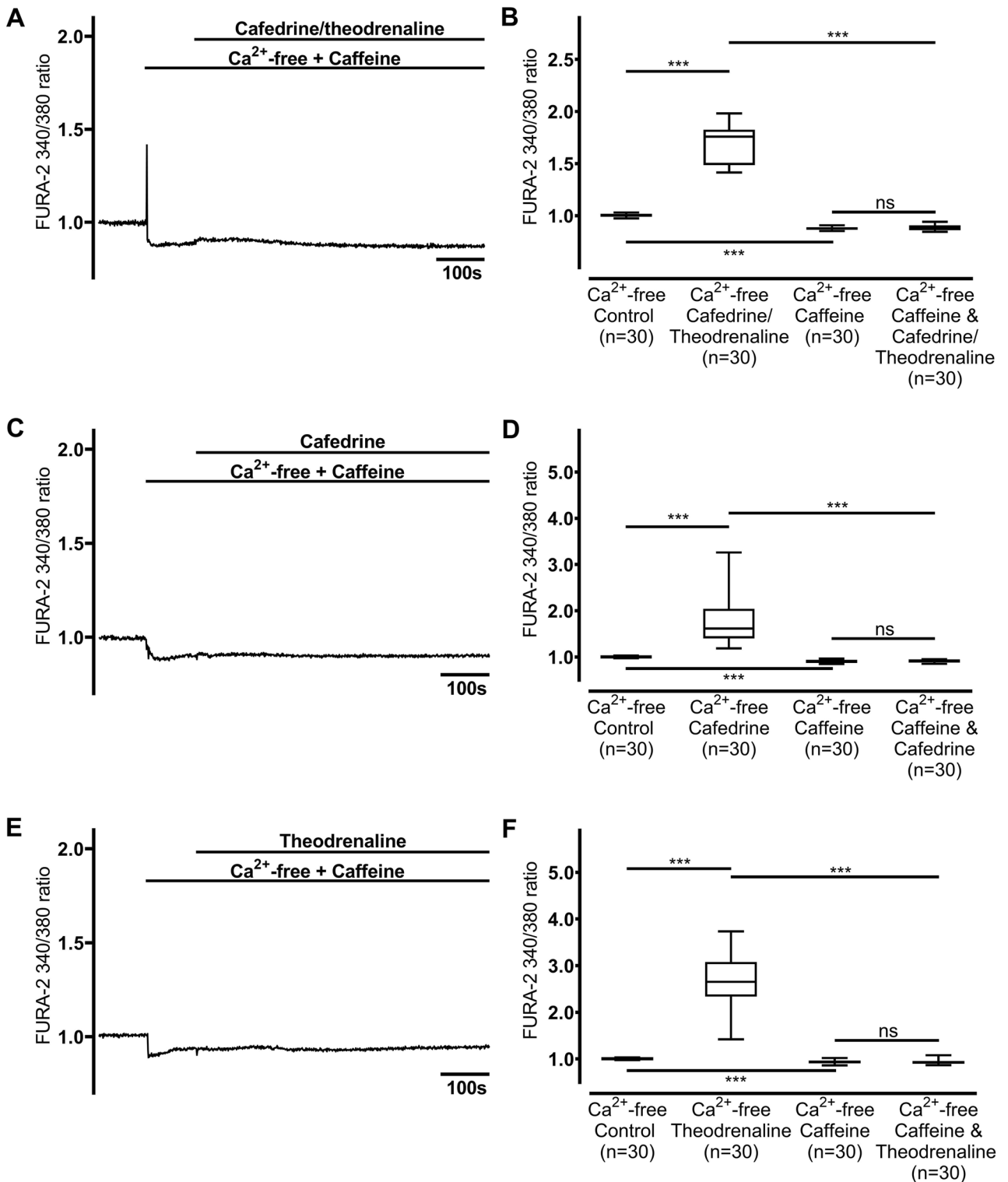
Figure 6. Ca^{2+} is released from intracellular caffeine-sensitive stores. When caffeine-sensitive stores were depleted by caffeine (30 mM), a subsequent decline in [Ca^2]$_i$ was observed, and no increase in [Ca^2]$_i$ was provoked by (**A, B**) 20:1 cafedrine/theodrenaline, (**C, D**) cafedrine alone, or (**E, F**) theodrenaline alone. The Ca^{2+}-free control group was represented by the same 30 cells in each chart. FURA-2 340/380 ratio was normalized after a 100-s resting period, and each group consists of 30 cells from at least three different coverslips, ensuring independent measurements. Scale bar width represents 100 s. n = number of individual cells, ***$p < 0.001$, ns: not significant, Wilcoxon rank sum test was used to test caffeine alone vs. drug preparation during inhibition, otherwise Mann–Whitney U test, adjusted α-level = 0.013. ⊥ SEM, box and whisker plots indicate median, interquartile range (box), minimum and maximum (whiskers).

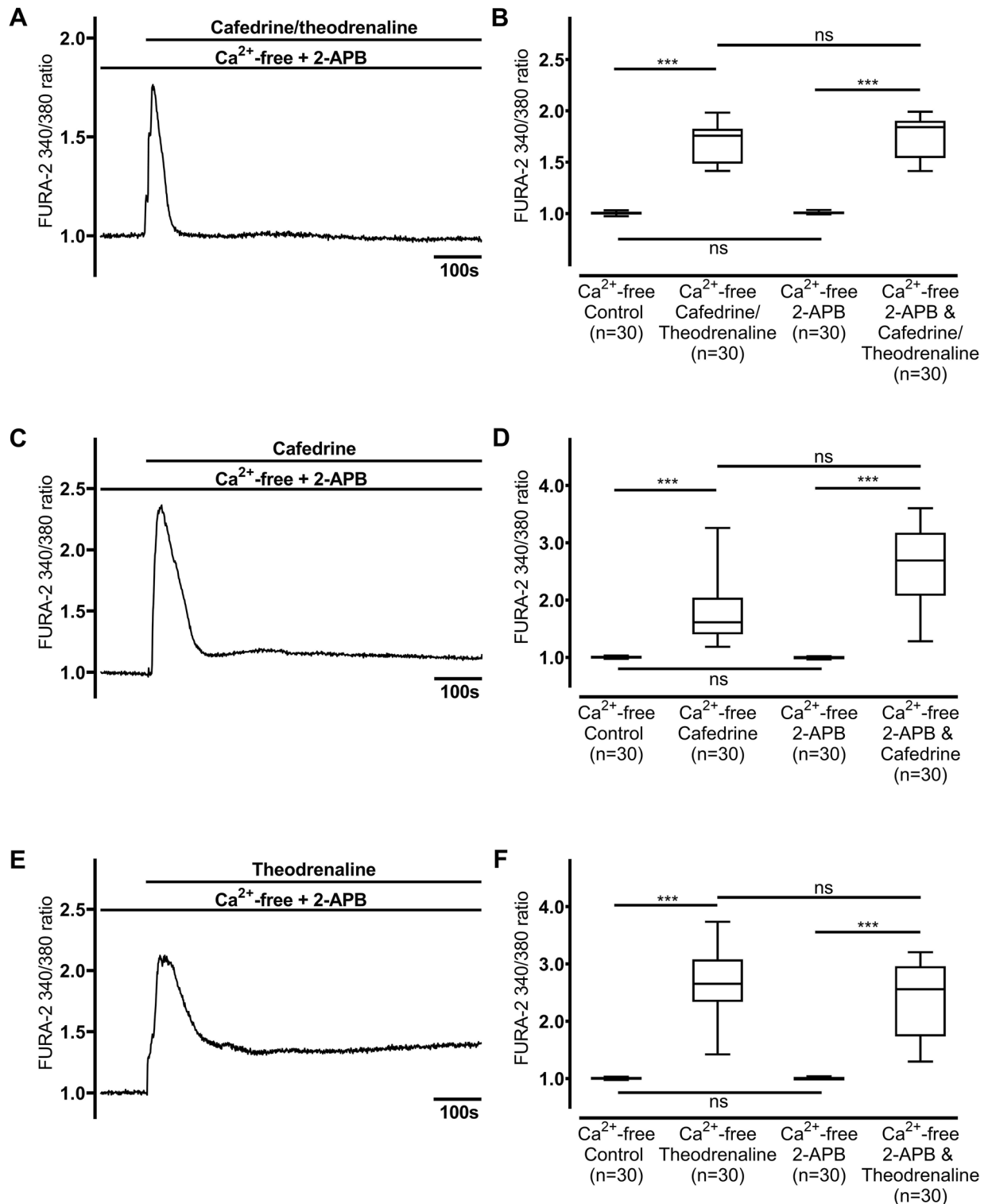**Figure 7.** Ca^{2+} release from intracellular stores occurs independently from IP_3 receptor activation. When IP_3 receptors were inhibited using 2-APB (40 μM), maximum $[Ca^2]_i$ increased equally after the application of (**A, B**) 20:1 cafedrine/theodrenaline, (**C, D**) cafedrine alone, and (**E, F**) theodrenaline alone. The Ca^{2+}-free control group was represented by the same 30 cells in each chart. FURA-2 340/380 ratio was normalized after a 100-s resting period, and each group consists of 30 cells from at least three different coverslips, ensuring independent measurements. Scale bar width represents 100 s. n = number of individual cells, ***$p < 0.001$, ns: not significant, Wilcoxon rank sum test was used to test 2-APB alone vs. drug preparation during inhibition, otherwise Mann–Whitney U test, adjusted α-level = 0.013. ⊥ SEM, box and whisker plots indicate median, interquartile range (box), minimum and maximum (whiskers).
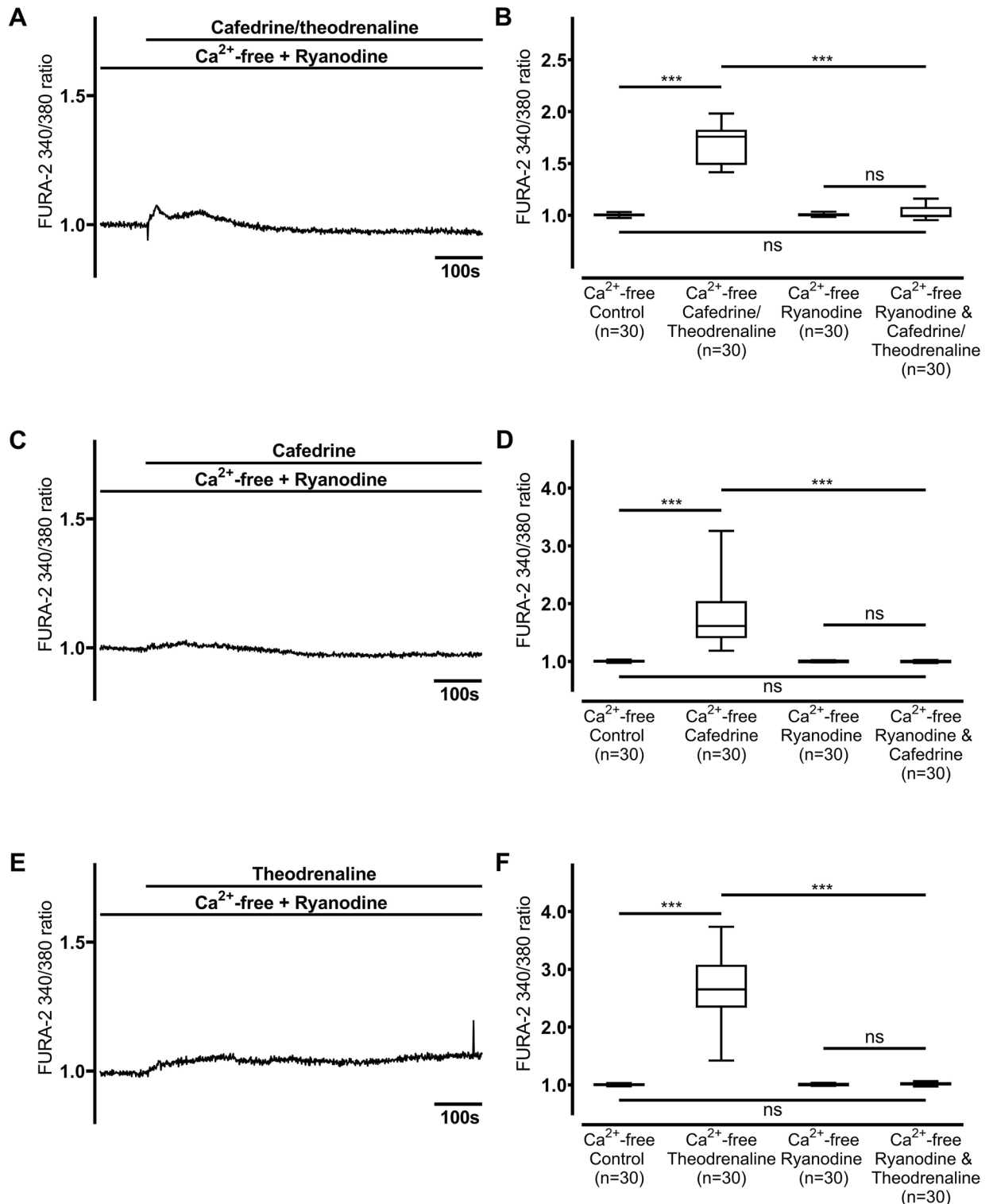
Figure 8. Ca^{2+} release from intracellular stores depends on ryanodine receptor activation. When ryanodine receptors were inhibited with ryanodine (40 μM), $[Ca^{2+}]_i$ remained unaltered after the application of (**A, B**) 20:1 cafedrine/theodrenaline, (**C, D**) cafedrine alone, and (**E, F**) theodrenaline alone. The Ca^{2+}-free control group was represented by the same 30 cells in each chart. FURA-2 340/380 ratio was normalized after a 100-s resting period, and each group consists of 30 cells from at least three different coverslips, ensuring independent measurements. Scale bar width represents 100 s. n = number of individual cells, ***$p < 0.001$, ns: not significant, Wilcoxon rank sum test was used to test ryanodine alone vs. drug preparation during inhibition, otherwise Mann–Whitney U test, adjusted α-level = 0.013. ⊥ SEM, box and whisker plots indicate median, interquartile range (box), minimum and maximum (whiskers).

release, RT-PCR was performed to identify the different RyR subtypes. Therefore, murine tracheae were used to ensure the availability of positive controls, ensuring accurate internal validity of the measurements.

Expression of RyR in murine tracheae

RyR-2 and *RyR-3* mRNA expression in both whole murine trachea and isolated tracheal epithelium (each n = 5) were identified by RT-PCR. *RyR-1* mRNA was not detected in the whole trachea or tracheal epithelium. An overview of the RT-PCR results, including the controls, is presented in Table 2, while Supplementary Fig. 1 illustrates the native PCR bands.

Discussion

Our experiments revealed that 20:1 cafedrine/theodrenaline, cafedrine alone, or theodrenaline alone increased $[Ca^{2+}]_i$, when applied to human tracheal epithelial cells. We observed sharp, transient peaks in the FURA-2 340/380 ratio, which followed a dose–response relationship and were described by the Hill equation. Herein, it should be noted that the effect curves of 20:1 cafedrine/theodrenaline and cafedrine alone showed a profile where the increase from 0 to 100% is already achieved within one log unit, which would be classically attributed to ion channel activation. In contrast, only the dose–response curve of theodrenaline clearly indicated receptor-mediated effects because the increase from 0 to 100% required two log units. However, although the formal criteria for receptor-mediated Ca^{2+} release were only barely met in our dose–response curves following the application of 20:1 cafedrine/theodrenaline and cafedrine alone, our following experiments clearly proved adrenergic and ryanodine receptor-mediated Ca^{2+} release following the application of all three substances analyzed in our experiments. Interestingly, the EC_{50} of cafedrine alone and theodrenaline alone were within comparable ranges; however, when applied as the clinically used 20:1 mixture, much more cafedrine was required to achieve a significant effect on $[Ca^{2+}]_i$, and the applied concentration of theodrenaline seemed almost negligible in the light of the calculated EC_{50} of theodrenaline alone. Moreover, $[Ca^{2+}]_i$ peaks observed after the application of 20:1 cafedrine/theodrenaline were consistently lower than those observed following applications of the individual substances alone. Interestingly, clinically irrelevant high concentrations of 20:1 cafedrine/theodrenaline ultimately led to cell lysis, which was also observed following the administration of high concentrations of cafedrine or theodrenaline alone; however we never observed a higher FURA-2 340/380 ratio than that shown in our dose–response curves. Although the pharmacokinetics of cafedrine and theodrenaline remain largely unknown, the immediate response in blood pressure was attributed to theodrenaline, while the effects of cafedrine were observed after a 20-min delay[17,20]. Therefore, it has been hypothesized that cafedrine may not provoke any sympathomimetic actions alone; it may be metabolized into active metabolites that exert its clinical effects[17]. In our experiments, the effect observed after the application of 20:1 cafedrine/theodrenaline could only be attributed to theodrenaline alone if strong synergistic effects would apply in the presence of cafedrine. Because the concentration of theodrenaline alone in the 20:1 mixture was insufficient to provoke any significant changes in $[Ca^{2+}]_i$, we conclude that the foremost effect on changing $[Ca^{2+}]_i$ in our experiments was induced by cafedrine. This assumption is supported by the observation that very high concentrations of cafedrine were applied using the 20:1 combination compared with the dose–response relationship of cafedrine alone. However, our model cannot represent the effects of potential drug metabolites, as we used isolated cells, and the drugs were directly applied to the buffer solution. Furthermore, clinical data reported a plasma concentration of 6 µg/ml after the intravenous application of one ampoule of 2 ml cafedrine/theodrenaline; therefore, all concentrations used in our experiments were significantly higher than clinically used concentrations[20]. However, the transient intravascular and intraepithelial concentrations immediately after injection are unknown and might be much higher than those observed after distribution to the body compartments; therefore, our data should be interpreted with caution, and further studies are necessary to evaluate the transferability of the concentrations used in our experiments.

After the transient peak, during which Ca^{2+} directly increases ciliary beat frequency and calmodulin-bound Ca^{2+} activated cyclic guanosine monophosphate (cGMP) and cyclic adenosine monophosphate (cAMP)-dependent pathways, $[Ca^{2+}]_i$ rapidly returned to its baseline[3]. The rapid restoration of baseline $[Ca^{2+}]_i$ is primarily explained by SERCA activity, which pumps Ca^{2+} into the ER after cytosolic Ca^{2+} release, or by mitochondrial Ca^{2+} buffering[21,22]. However, almost every other small cell organelle contributes to the rapid restoration of baseline $[Ca^{2+}]_i$, and prolonged alteration of ciliary beat frequency is induced by transient changes in $[Ca^{2+}]_i$. Immediately after purinergic or cholinergic stimulation, tracheal epithelial cells exhibited a transient increase in $[Ca^{2+}]_i$; however, ciliary beat frequency remained consistently increased[23,24]. Therefore, we conclude that

	Ryr1	*Ryr2*	*Ryr3*
Skeletal muscle	+	−	+
Cardiac muscle	−	+	−
Diaphragm	+	−	+
Whole trachea	−	+	+
Tracheal epithelium	−	+	+
Negative control (H_2O)	−	−	−

Table 2. RT-PCR identified ryanodine receptor (RyR)-2 and RyR-3 in murine whole trachea and tracheal epithelium.

analogous mechanisms are mediated after the stimulation of β-adrenergic receptors, which were the pivotal receptors involved in $[Ca^{2+}]_i$ alterations in our experiments. The increase in $[Ca^{2+}]_i$ completely vanished after 20:1 cafedrine/theodrenaline, cafedrine alone, or theodrenaline alone were added during non-selective adrenergic receptor inhibition. These results are in line with the clinical effect of cafedrine/theodrenaline, which increases cardiac stroke volume via $β_1$-adrenergic receptor activation[14]. In-vitro studies using human atrial myocardium and coronary arteries also elucidated $β_1$-adrenergic receptor activation as a pivotal mechanism; however, effects on α-adrenergic receptors were observed in arteries after β-adrenergic receptor inhibition[17,25]. Although these effects were attributed to theodrenaline alone, we did not observe similar effects in human tracheal epithelial cells. These observations are in line with the data reported by Weiterer et al., who reported the exclusive presence of the α1D-adrenergic receptor subtype in murine tracheal epithelium[26]. However, murine particle transport velocity was independent from α-adrenergic receptor activation. Therefore, we conclude that α-receptor activation might occur in human tracheal epithelial cells following the administration of cafedrine/theodrenaline, but no influence on $[Ca^{2+}]_i$ or mucociliary clearance could be detected in light of the available in-vitro data[26]. The theophylline component of cafedrine and theodrenaline is believed to inhibit PDE, which should lead to the persistence of second messengers, such as cGMP and cAMP, improving cardiac inotropy[14]. However, only high, clinically irrelevant concentrations of cafedrine/theodrenaline were able to provoke significant inhibition of PDE in human atrial myocardium[17]. Although we used high concentrations of cafedrine/theodrenaline, cafedrine alone, and theodrenaline alone, we were only able to detect β-adrenergic receptor stimulation because the increase in $[Ca^{2+}]_i$ completely vanished in the presence of β-adrenergic receptor inhibition. When other signal transduction cascades were involved, we should have detected a persistent increase in $[Ca^{2+}]_i$. This finding is underlined by the knowledge that PDE inhibition might not influence ciliary beat frequency or mucociliary clearance to a clinically relevant degree, because data remain controversial regarding the alteration of mucociliary clearance following treatment with theophylline[27–29].

When we used Ca^{2+}-free buffer solution, $[Ca^{2+}]_i$ increased to a significantly lesser degree following administration of cafedrine alone and theodrenaline alone than the increase observed in Ca^{2+}-containing buffer solution. Therefore, extracellular Ca^{2+} influx contributes to the rise in $[Ca^{2+}]_i$, which is foremost realized through SOCE in non-excitable cells following Ca^{2+} release from internal stores[12,13]. ORAI proteins, which are mediated by stromal interaction molecule proteins, are the most important mediators of SOCE[12]. Therefore, further experiments elucidating receptor expression and distinct signal transduction pathways should be performed, although their specific inhibition is complicated due to their diverse interactions and multiple targets located on the plasma membrane[13]. However, because the $[Ca^{2+}]_i$ peak in the Ca^{2+}-free buffer solution was comparable to the peak observed in Ca^{2+}-containing buffer solution following the administration of 20:1 cafedrine/theodrenaline, the clinical relevance of SOCE following the administration of cafedrine/theodrenaline in human tracheal epithelial cells remains questionable. Internal stores were depleted to detect the intracellular stores, which released Ca^{2+} following the administration of cafedrine/theodrenaline. When mitochondrial Ca^{2+} stores were depleted, $[Ca^{2+}]_i$ continued to increase following the administration of 20:1 cafedrine/theodrenaline, cafedrine alone, or theodrenaline alone. Therefore, we conclude that cafedrine/theodrenaline does not depolarize mitochondrial membrane potential, which would lead to Ca^{2+} release from these stores. However, $[Ca^{2+}]_i$ peaks following the administration of 20:1 cafedrine/theodrenaline and cafedrine alone were significantly higher than those observed without prior mitochondrial store depletion. This observation confirms the mitochondrial ability to buffer Ca^{2+} ions via the mitochondrial Ca^{2+} uniporter when $[Ca^{2+}]_i$ exceeds 500 nM[30]. Interestingly, $[Ca^{2+}]_i$ remained higher for the rest of the observation time. Because DNP administration decouples oxidative phosphorylation without altering cytosolic pH, less ATP supplying the ATP-dependent SERCA might be available in these experiments, leading to the observation of persistent $[Ca^{2+}]_i$ baseline shift. However, SERCA was still able to handle the transient peak $[Ca^{2+}]_i$ by altering $[Ca^{2+}]_i$ close to its former baseline value. This finding underlines our conclusion that the elevated peak in $[Ca^{2+}]_i$ is foremost triggered by the inhibited mitochondrial Ca^{2+} capacity and not by a lack of ATP, which might impair SERCA activity.

Because the increase in $[Ca^{2+}]_i$ completely vanished following the administration of 20:1 cafedrine/theodrenaline, cafedrine alone, or theodrenaline alone, when RyR were inhibited, we conclude that cafedrine/theodrenaline releases Ca^{2+} from the ER exclusively by RyR activation. In general, Ca^{2+} release from the ER is achieved via IP_3 receptor or RyR activation[31]. However, our experiments revealed equal peaks of $[Ca^{2+}]_i$ when IP_3 receptors were inhibited, and the increase in $[Ca^{2+}]_i$ completely vanished after RyR inhibition. Therefore, we conclude that Ca^{2+} release following β-adrenergic receptor activation depends solely on RyR activation, and IP_3 receptor-associated Ca^{2+} release does not occur in human tracheal epithelial cells following cafedrine/theodrenaline administration.

Consequently, RyR-2 and RyR-3 expression was revealed using RT-PCR in murine tracheal epithelium. While RyR-3 is co-expressed with RyR-1 or RyR-2 in many tissues, RyR 2 has mainly been studied in cardiac muscle cells; however, RyR-2 expression has been demonstrated in smooth muscle cells and non-excitable cells, such as pancreatic acinar cells and kidney epithelial cells[32–35]. Therefore, RyR-2 expression in the tracheal epithelium is in line with its expression in other non-excitable cells. While RyR activation is achieved following various signal transduction cascades, the best-known mechanism is the Ca^{2+}-induced Ca^{2+}-release, whereby RyR-2 activation is triggered by a local increase of $[Ca^{2+}]_i$[36]. Local increase in $[Ca^{2+}]_i$ can be realized through nearby RyR activation, or IP_3 receptor activation; however, our data indicate that RyR activation was independent from IP_3 receptor activation following cafedrine/theodrenaline administration[37]. Therefore, alternative RyR activation following β-adrenergic receptor stimulation must be considered in tracheal epithelial cells. β-adrenergic stimulation has been shown to increase RyR-2 activity in cardiac muscle cells via intracellular-mediated Ca^{2+} and Mg^{2+} regulation, and receptor phosphorylation[38]. Furthermore, protein kinase A and cAMP, which are both pivotal messengers following the $β_1$-signal transduction cascade, have been shown to induce Ca^{2+} release via RyR-2 in cardiac muscles and non-excitable cells, respectively[39,40]. In addition, adrenergic receptor signaling increases nicotinic acid adenine dinucleotide phosphate and cyclic adenosine diphosphate-ribose levels, which

both activate RyR-2-associated Ca^{2+} release[33,41]. Because RyR-3 is more readily activated by an increase in local $[Ca^{2+}]_i$ compared with RyR-2, its activation in tracheal epithelial cells following the administration of cafedrine/theodrenaline can be achieved following RyR 2-associated Ca^{2+} efflux[42]. However, as discrepancies in receptor expression between mammals could not be excluded, further studies in human tissues should be conducted to confirm RyR expression. Local distribution, and the RyR-2-to-RyR-3 ratio in tracheal epithelial cells could be evaluated using immunohistochemistry.

Several limitations of our experiments must be acknowledged. First, we used isolated tracheal epithelial cells; therefore, the physiological integrity of a respiratory tract was not preserved, including a lack of basal tissues and cell–cell junctions. Therefore, physiological drug administration via capillary vessels could not be replicated, and atypical entrance (e.g. from the apical or lateral side of the cells) of our tested drugs was preserved. Second, we used high concentrations of cafedrine/theodrenaline, cafedrine, and theodrenaline to achieve alterations in $[Ca^{2+}]_i$ and clinically administered concentrations are much lower; therefore, it is possible that we observed $[Ca^{2+}]_i$ kinetics that do not occur when lower concentrations are used in vivo. Third, some concentrations applied to achieve the specific dose–response curves were higher than was warranted by the integrity of the observed cells; therefore, a maximum FURA-2 340/380 ratio following substance administration was set at the last valid observed value. However, concentrations applied to assess the distinct signal transduction cascades did prove the validity of the calculated dose–response curves in our experimental setting. Fourth, our measurement of $[Ca^{2+}]_i$ using the FURA-2 340/380 ratio was not calibrated; therefore, we can only report relative alterations in $[Ca^{2+}]_i$, and no absolute concentrations were measured.

In conclusion, we provide evidence that cafedrine/theodrenaline, cafedrine alone, or theodrenaline alone induce the release of Ca^{2+} from caffeine-sensitive internal stores that is exclusively triggered by β-adrenergic receptor stimulation, resulting in RyR activation. RT-PCR revealed the presence of RyR-2 and RyR-3 in mammalian cells, and the relevant influence of extracellular Ca^{2+} influx was only observed after the application of cafedrine alone or theodrenaline alone. However, clinical plasma concentrations are considerably lower than those used in our experiments to trigger a significant increase in $[Ca^{2+}]_i$; therefore, further studies are needed to alter the ability of cafedrine/theodrenaline to change mucociliary clearance in clinical practice.

Data availability
The datasets used and/or analysed during the current study are available from the corresponding author on reasonable request.

References
1. Legendre, M., Zaragosi, L. E. & Mitchison, H. M. Motile cilia and airway disease. *Semin Cell Dev Biol.* **110**, 19–33. https://doi.org/10.1016/j.semcdb.2020.11.007 (2021).
2. Whitsett, J. A. Airway epithelial differentiation and mucociliary clearance. *Ann. Am. Thorac. Soc.* https://doi.org/10.1513/AnnalsATS.201802-128AW (2018).
3. Schmid, A. & Salathe, M. Ciliary beat co-ordination by calcium. *Biol. Cell.* **103**, 159–169. https://doi.org/10.1042/bc20100120 (2011).
4. Delmotte, P. & Sanderson, M. J. Ciliary beat frequency is maintained at a maximal rate in the small airways of mouse lung slices. *Am. J. Respir. Cell Mol. Biol.* **35**, 110–117. https://doi.org/10.1165/rcmb.2005-0417OC (2006).
5. Lee, R. J. & Foskett, J. K. Ca2+ signaling and fluid secretion by secretory cells of the airway epithelium. *Cell Calcium.* https://doi.org/10.1016/j.ceca.2014.02.001 (2014).
6. Peng, W., Wong, Y. C. & Krainc, D. Mitochondria-lysosome contacts regulate mitochondrial Ca2+ dynamics via lysosomal TRPML1. *Proc. Natl. Acad. Sci. U. S. A.* **117**, 19266–19275. https://doi.org/10.1073/pnas.2003236117 (2020).
7. Galaz-Montoya, M., Wright, S. J., Rodriguez, G. J., Lichtarge, O. & Wensel, T. G. β2-Adrenergic receptor activation mobilizes intracellular calcium via a non-canonical cAMP-independent signaling pathway. *J. Biol. Chem.* **292**, 9967–9974. https://doi.org/10.1074/jbc.M117.787119 (2017).
8. Ribeiro, C. M. P., Paradiso, A. M., Livraghi, A. & Boucher, R. C. The mitochondrial barriers segregate agonist-induced calcium-dependent functions in human airway epithelia. *J. Gen. Physiol.* **122**, 377–387. https://doi.org/10.1085/jgp.200308893 (2003).
9. Duchen, M. R. Mitochondria and calcium: From cell signalling to cell death. *J. Physiol.* https://doi.org/10.1111/j.1469-7793.2000.00057.x (2000).
10. Medina, D. L. Lysosomal calcium and autophagy. *Int. Rev. Cell Mol. Biol.* https://doi.org/10.1016/bs.ircmb.2021.03.002 (2021).
11. Sargsyan, Y. *et al.* Peroxisomes contribute to intracellular calcium dynamics in cardiomyocytes and non-excitable cells. *Life Sci. Alliance.* https://doi.org/10.26508/LSA.202000987 (2021).
12. Nguyen, N. T. *et al.* Store-operated calcium entry mediated by ORAI and STIM. *Compr. Physiol.* **8**, 981–1002. https://doi.org/10.1002/cphy.c170031 (2018).
13. Spinelli, A. M. & Trebak, M. Orai channel-mediated Ca2+ signals in vascular and airway smooth muscle. *Am. J. Physiol. - Cell Physiol.* **310**, C402–C413. https://doi.org/10.1152/ajpcell.00355.2015 (2016).
14. Bein, B., Christ, T. & Eberhart, L. H. J. Cafedrine/theodrenaline (20:1) is an established alternative for the management of arterial hypotension in germany-a review based on a systematic literature search. *Front. Pharmacol.* **8**, 68. https://doi.org/10.3389/fphar.2017.00068 (2017).
15. Weitzel, M., Hammels, P., Schorer, C., Klingler, H. & Weyland, A. Hemodynamic effects of cafedrine/theodrenaline on anesthesia-induced hypotension. *Anaesthesist* **67**, 766–772. https://doi.org/10.1007/s00101-018-0472-z (2018).
16. Heller, A. R., Heger, J., de Gama, A. M. & Müller, M. P. Cafedrine/theodrenaline in anaesthesia: Influencing factors in restoring arterial blood pressure. *Anaesthesist* **64**, 190–6. https://doi.org/10.1007/s00101-015-0005-y (2015).
17. Kloth, B. *et al.* Akrinor™, a cafedrine/theodrenaline mixture (20:1), increases force of contraction of human atrial myocardium but does not constrict internal mammary artery in vitro. *Front. Pharmacol.* https://doi.org/10.3389/fphar.2017.00272 (2017).
18. Eberhart, L. *et al.* A non-interventional comparative study of the 20:1 combination of cafedrine/theodrenaline versus ephedrine for the treatment of intra-operative arterial hypotension: the 'HYPOTENS' study design and rationale. *Curr. Med. Res. Opin.* **34**, 953–961. https://doi.org/10.1080/03007995.2018.1438379 (2018).

19. Kranke, P. *et al.* Treatment of spinal anaesthesia-induced hypotension with cafedrine/theodrenaline versus ephedrine during caesarean section: Results from HYPOTENS, a national, multicentre, prospective, noninterventional study. *Eur. J. Anaesthesiol.* **38**, 1067–1076. https://doi.org/10.1097/EJA.0000000000001474 (2021).

20. Sternitzke, N., Schieffer, H., Rettig, G. & Bette, L. Die Beeinflussung der Herz-Kreislauf-Dynamik durch die Theophyllin-Verbindung Cafedrin und Theodrenalin sowie durch ihre Kombination. *Herz Kreislauf.* **8**, 401–412 (1984).

21. Roux, E. & Marhl, M. Role of sarcoplasmic reticulum and mitochondria in Ca2+ removal in airway myocytes. *Biophys. J.* **86**, 2583–2595. https://doi.org/10.1016/S0006-3495(04)74313-1 (2004).

22. Berridge, M. J., Lipp, P. & Bootman, M. D. The versatility and universality of calcium signalling. *Nat. Rev. Mol. Cell Biol.* https://doi.org/10.1038/35036035 (2000).

23. Lieb, T., Frei, C. W., Frohock, J. I., Bookman, R. J. & Salathe, M. Prolonged increase in ciliary beat frequency after short-term purinergic stimulation in human airway epithelial cells. *J. Physiol.* **538**, 633–646. https://doi.org/10.1113/jphysiol.2001.013222 (2002).

24. Salathe, M. & Bookman, R. J. Mode of Ca2+ action on ciliary beat frequency in single ovine airway epithelial cells. *J. Physiol.* **520**, 851–865. https://doi.org/10.1111/j.1469-7793.1999.00851.x (1999).

25. Usichenko, T. I. *et al.* Akrinor-induced relaxation of pig coronary artery in vitro is transformed into α1-adrenoreceptor-mediated contraction by pretreatment with propranolol. *J. Cardiovasc. Pharmacol.* **47**, 450–455. https://doi.org/10.1097/01.fjc.0000211710.87863.89 (2006).

26. Weiterer, S. *et al.* Galactomannan and zymosan block the epinephrine-induced particle transport in tracheal epithelium. *PLoS One.* **10**, e0143163. https://doi.org/10.1371/journal.pone.0143163 (2015).

27. Matthys, H. & Kohler, D. Effect of theophylline on mucociliary clearance in man. *Eur. J. Respir. Dis.* **61**, 98–102 (1980).

28. Ziment, I. Theophylline and Mucociliary clearance. *Chest.* **92**, 38S-43S. https://doi.org/10.1378/chest.92.1_supplement.38s (1987).

29. Konrad, F., Schreiber, T., Hahnel, J., Kilian, J. & Georgieff, M. The effect of theophylline on the mucociliary clearance function in ventilated intensive care patients. *Anaesthesist* **43**, 101–106. https://doi.org/10.1007/s001010050038 (1994).

30. Henrich, M. & Buckler, K. J. Effects of anoxia and aglycemia on cytosolic calcium regulation in rat sensory neurons. *J. Neurophysiol.* **100**, 456–473. https://doi.org/10.1152/jn.01380.2007 (2008).

31. Woll, K. A. & Van Petegem, F. Calcium-release channels: Structure and function of IP3 receptors and ryanodine receptors. *Physiol. Rev.* https://doi.org/10.1152/PHYSREV.00033.2020 (2022).

32. Tunwell, R. E. A. & Lai, F. A. Ryanodine receptor expression in the kidney and a non-excitable kidney epithelial cell. *J. Biol. Chem.* **271**, 29583–29588. https://doi.org/10.1074/jbc.271.47.29583 (1996).

33. Yamaguchi, N. Molecular insights into calcium dependent regulation of ryanodine receptor calcium release channels. *Adv. Exp. Med. Biol.* https://doi.org/10.1007/978-3-030-12457-1_13 (2020).

34. Sutko, J. L. & Airey, J. A. Ryanodine receptor Ca2+ release channels: Does diversity in form equal diversity in function?. *Physiol. Rev.* https://doi.org/10.1152/physrev.1996.76.4.1027 (1996).

35. Bennett, D. L. *et al.* Expression and function of ryanodine receptors in nonexcitable cells. *J. Biol. Chem.* **271**, 6356–6362. https://doi.org/10.1074/jbc.271.11.6356 (1996).

36. Ozawa, T. Ryanodine-sensitive Ca2+ release mechanism in non-excitable cells (review). *Int. J. Mol. Med.* https://doi.org/10.3892/ijmm.7.1.21 (2001).

37. Essin, K. & Gollasch, M. Role of ryanodine receptor subtypes in initiation and formation of calcium sparks in arterial smooth muscle: Comparison with striated muscle. *J. Biomed. Biotechnol.* https://doi.org/10.1155/2009/135249 (2009).

38. Li, J. *et al.* ß-Adrenergic Stimulation Increases RyR2 Activity via Intracellular Ca2+ and Mg2+ Regulation. *PLoS One* https://doi.org/10.1371/journal.pone.0058334 (2013).

39. Bovo, E., Huke, S., Blatter, L. A. & Zima, A. V. The effect of PKA-mediated phosphorylation of ryanodine receptor on SR Ca2 + leak in ventricular myocytes. *J. Mol. Cell Cardiol.* **104**, 9–16. https://doi.org/10.1016/j.yjmcc.2017.01.015 (2017).

40. Ozawa, T. Cyclic AMP induces ryanodine-sensitive Ca2+ release from microsomal vesicles of rat parotid acinar cells. *Biochem. Biophys. Res. Commun.* **246**, 422–425. https://doi.org/10.1006/bbrc.1998.8636 (1998).

41. Lewis, A. M. *et al.* ß-Adrenergic receptor signaling increases NAADP and cADPR levels in the heart. *Biochem. Biophys. Res. Commun.* **427**, 326–329. https://doi.org/10.1016/j.bbrc.2012.09.054 (2012).

42. Ogawa, Y., Kurebayashi, N. & Murayama, T. Putative roles of Type 3 ryanodine receptor isoforms (RyR3). *Trends Cardiovasc. Med.* https://doi.org/10.1016/S1050-1738(00)00050-5 (2000).

Acknowledgements

Author contributions

G.S.: Conceptualization, Data curation, Formal analysis, Investigation, Writing—original draft; G.R.: Data curation, Formal analysis, Investigation, Visualization, Writing—review & editing; S.M.: Formal analysis, Investigation, Visualization, Writing—review & editing; K.R.: Formal analysis, Investigation, Writing—review & editing; M.S.: Conceptualization, Project administration, Writing—review & editing; C.K.: Conceptualization, Validation, Writing—review & editing; M.H.: Conceptualization, Validation, Writing—review & editing.

Funding

Competing interests

Additional information

Supplementary Information The online version contains supplementary material available at https://doi.org/10.1038/s41598-023-43342-0.

Correspondence and requests for materials should be addressed to G.S.

Reprints and permissions information is available at www.nature.com/reprints.